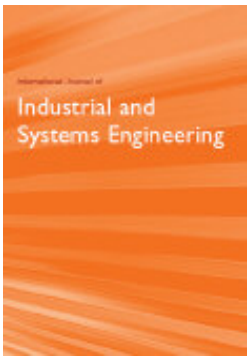


**International Journal of Industrial and Systems Engineering**

ISSN online: 1748-5045 - ISSN print: 1748-5037
https://www.inderscience.com/ijise

# A robust non-singular fast terminal sliding mode controller for optimising a wind energy process

Karim Dahech, Moez Allouche, Tarak Damak

**DOI:** 10.1504/IJISE.2022.10048717

**Article History:**
Received: 09 July 2021
Accepted: 29 May 2022
Published online: 08 January 2024

# A robust non-singular fast terminal sliding mode controller for optimising a wind energy process

Karim Dahech*, Moez Allouche and Tarak Damak

Laboratory of Sciences and Techniques of Automatic Control and Computer Engineering (Lab-STA),
National School of Engineering of Sfax (ENIS),
University of Sfax,
P.O. Box 1173, 3038 Sfax, Tunisia
Email: dahechkarim@yahoo.fr
Email: moez_allouche@yahoo.fr
Email: tarak.damak@enis.rnu.tn
*Corresponding author

**Abstract:** This paper deals with the development of a non-singular fast terminal sliding mode controller for maximum power point tracking of wind energy conversion system. The studied system is made up of a wind turbine coupled to a permanent magnet synchronous generator, a three-phase diode rectifier and supplying through a boost converter, a resistive load. The principle of the control scheme is based on electrical measurements and the choice of a suitable sliding surface. This approach presents a good transition response, a low tracking error and a very fast reaction against wind speed variations compared to the traditional sliding mode controller. The effectiveness of the proposed control scheme is demonstrated by numerical simulations under different climatic conditions.

**Keywords:** wind energy process; maximum power point tracking; robust control; non-singular fast terminal sliding mode controller; Lyapunov function.

**Reference** to this paper should be made as follows: Dahech, K., Allouche, M. and Damak, T. (2024) 'A robust non-singular fast terminal sliding mode controller for optimising a wind energy process', *Int. J. Industrial and Systems Engineering*, Vol. 46, No. 1, pp.107–125.

**Biographical notes:** Karim Dahech received his Electrical Engineering Diploma from the National School of Engineers of Gabes, Tunisia in 2002, the MSc degree in Automatic and Industrial Data Processing, and the PhD degree in Electrical Engineering from the National School of Engineers of Sfax, Tunisia in 2004 and 2009, respectively. He is currently an Assistant Professor of Electrical Engineering in the Higher Institute of Industrial Management of Sfax. His research interests include modelling, estimation and control of nonlinear systems.

Moez Allouche received his MSc degree from National Engineering School of Sfax, Tunisia in 2006. He obtained the PhD degree in Electrical Engineering from the National Engineering School of Sfax, Tunisia in 2010. Currently, he is an Associate Professor in the National Engineering School of Sfax. His research interests include, on the theoretical side, analysis and control of

fuzzy/LPV polytopic models, multiple model approach, robust control, fault detection and isolation (FDI), fault tolerant control (FTC), analysis and control via LMI optimisation techniques and Lyapunov methods. On the application side he is mainly interested in renewable energy.

Tarak Damak received his Diploma in Electrical Engineering from the National School of Engineers of Sfax, Tunisia, in 1989 and his DEA degree in Automatic Control from the Institut National des Sciences Appliquées de Toulouse, France, in 1990. He received his PhD from the Université Paul Sabatier de Toulouse, France, in 1994. In 2006, he then obtained the University Habilitation from the National School of Engineers of Sfax. He is currently a Professor in the Department of Mechanical Engineering of the National School of Engineers of Sfax, Tunisia. His current research interests are in the fields of distributed parameter systems, sliding mode control and observers, adaptive nonlinear control.

## 1 Introduction

Electricity represents a main factor for the economic development of countries. The need for comfort, industrialisation and technological progress are increasing the importance of electricity. Therefore, this factor is considered to be an indicator for measuring the level of development and translating the quality of life in a country. For a long time, the generation of electric energy relies mainly on fossil resources which take a large part of carbon monoxide emissions. However, these resources cause excessive release of greenhouse gases and are involved in global warming. Therefore it is essential to find remedies for these problems and to look for alternative solutions to replace these reserves (Zhuo et al., 2016; Kumar and Selvakumar, 2020).

Nowadays, renewable energies are becoming widely adapted to the production of electricity. This kind of inexhaustible energy allows a generation of electricity less dependent on resources and without harming the environment (Gam et al., 2019; Xiong et al., 2020). Wind energy is currently the most competitive source among the various forms of renewable energy adopted for the production of electricity. Two techniques are available for regulating the power delivered by wind turbines: either mechanically by varying the angles of the blades or electrically by varying the electrical magnitudes. The first method is expensive and requires regular maintenance. However, the latter is more reliable and requires less maintenance (Hau, 2013). Several types of electric generators are used in wind power applications. In this context, synchronous generators prove their efficiency in several works. They have the advantage of being connected directly to the turbine without the need for a gearbox. In addition, electronic converters are used in wind system applications not only to allow the system to operate at variable speed but also to extract the optimum power supplied.

To improve the efficiency of a wind energy conversion system, many researchers have proposed various maximum power point tracking (MPPT) algorithms. Kumar and Chatterjee (2016), Jayshree et al (2021) and Abdullah et al. (2012) presented a literature review on conventional and advanced MPPT approaches. The advantages, disadvantages and complete comparison of different MPPT methods are discussed in terms of complexity, necessity of wind speed measurement, response time, efficiency under variable wind profile, and also ability to acquire producing maximum power.

Daili et al. (2015) developed a new perturbation and observation (P&O) MPPT algorithm to solve some problems related to the conventional P&O like rapidity, efficiency, divergence, etc... Kesraoui et al. (2011) used a proportional integral (PI) regulator for an optimal extraction of output power from grid connected variable speed wind energy conversion system. Nasiri et al. (2014) have been shown that the optimal torque control method is more efficient and has obviously good performance in maximum power point tracking then the tip speed ratio method. A T-S fuzzy MPPT control is presented in (Chiu CS et al., 2013; Allouche et al.,2019; Abderrahim et al., 2020,2021). Recently, several authors (Ardjal et al., 2018; Yin et al., 2020; Hostettler and Wang, 2015; Evangelista et al., 2017; Abolvafaei and Ganjefar, 2019, 2020; Yazici and Yaylaci, 2019; Yin et al., 2015; Ruban periyanayagam and Joo, 2022) have proposed some MPPT approaches based on the sliding mode theory.

In this paper a nonsingular fast terminal sliding mode controller (NFTSMC) is proposed for maximum power point tracking. The control law is applied to a wind energy conversion system (WECS) composed of a wind turbine, a permanent magnet synchronous generator (PMSG), an uncontrolled rectifier, a DC-DC boost converter and a resistive load.

Compared to other recent works, the main contributions of this study can be summarised in three points:

1 the proposed control scheme does not require mechanical sensors

2 convergence is ensured in a finite time

3 a robust tracking is ensured as shown in the analysis using the Lyapunov stability theorem.

The remainder of the paper is organised into four Sections: Section 2 gives a general description of the considered WECS with the mathematical model of each element of the system. The design of the proposed MPPT algorithm is introduced in Section 3. Section 4 illustrates some simulation results. Finally, Section 5 summarises the results of this work and draws conclusions.

## 2 System description

Figure 1 outlines the configuration of the WECS considered in this study. The system is made up of a wind turbine, a PMSG, a diode rectifier, a DC-DC boost converter and it supply a resistive load.

In order to study the wind energy conversion system and synthesise MPPT control algorithm, it is essential to mathematically model the different elements of this system.

**Figure 1** WECS configuration (see online version for colours)

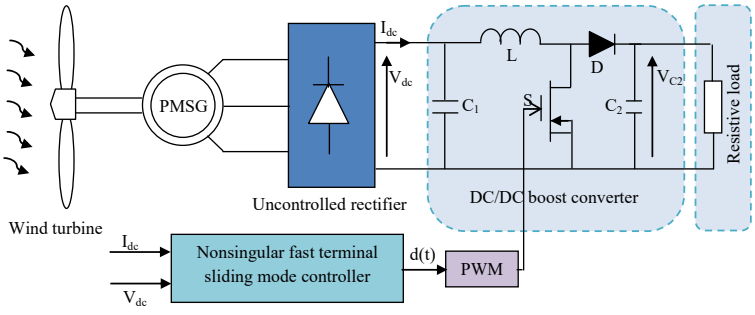


## 2.1 Wind turbine model

The aerodynamic power extracted from the wind by a turbine is expressed by Mousa et al. (2020):

$$P_w = \frac{1}{2}\rho\pi R^2 V_w{}^3 C_p(\lambda) \tag{1}$$

where $\rho$ in the air density, $R$ is the blade length, $V_w$ represents the wind speed and defines the aerodynamic power coefficient generally expressed as a function of the tip speed ratio given by Mousa et al. (2020):

$$C_p(\lambda) = 0.5176\left(\frac{116}{\lambda_i} - 0.4\beta - 5\right)\exp\left(-\frac{21}{\lambda_i}\right) + 0.0068\lambda \tag{2}$$

$$\frac{1}{\lambda_i} = \frac{1}{\lambda + 0.08\beta} - \frac{0.055}{\beta^2 + 1} \tag{3}$$

where $\beta$ is the pitch angle of the blades whose value is kept at zero in this work. The tip speed ratio $\lambda$ is given as follows (Mousa et al., 2020):

$$\lambda = \frac{R\omega_m}{V_w} \tag{4}$$

where $\omega_m$ is the mechanical angular shaft speed. By neglecting the mechanical and electrical losses, the mechanical torque available on the shaft of the wind turbine can be expressed as follows:

$$T_w = \frac{P_w}{\omega_m} = \frac{1}{2}\rho\pi R^2 V_w{}^3 C_p(\lambda) \Big/ \omega_m \tag{5}$$

Figure 2 shows the evolution of the aerodynamic power as a function of the generator speed for different values of wind speed. As can be seen from these figures, for each wind speed, there is an optimum rotor speed that gives maximum power recovered by the turbine. The $C_p(\lambda)$ curve is illustrated in Figure 3. From the figure, we can conclude that there is a single optimal point $\lambda_{opt} = 6.9$ for $C_p$ to reach its maximum value $C_{pmax} = 0.47$.

**Figure 2** Characteristics $P_w = f(\omega_m)$ (see online version for colours)

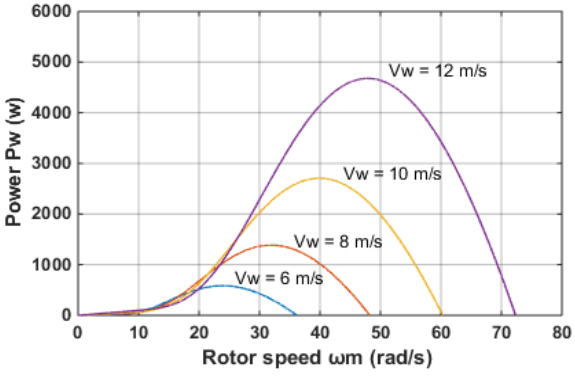


**Figure 3** $C_p(\lambda)$ curve (see online version for colours)

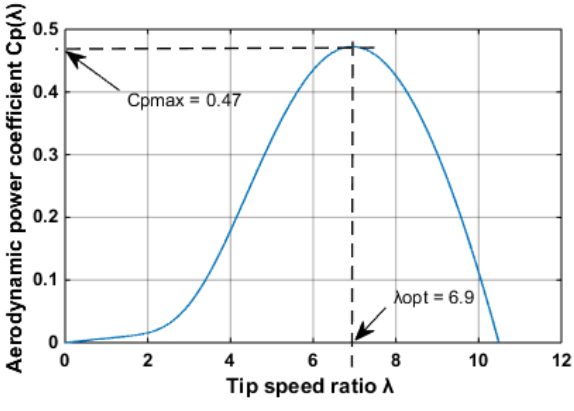


## *2.2 Permanent magnet synchronous generator model*

The PMSG is used to convert the mechanical power produced by the rotation of the blades of the wind turbine into electrical energy. By neglecting the coefficient of friction in the mechanical equation, the dynamic behaviour of the PMSG can be represented in the $d_q$ synchronous rotating reference frame by the following equations (Chiu et al., 2014).

$$\frac{di_{sd}}{dt} = -\frac{R_s}{L_s} i_{sd} + n_p \omega_m i_{sq} - \frac{V_s i_{sd}}{L_s \sqrt{{i_{sd}}^2 + {i_{sq}}^2}} \tag{6}$$

$$\frac{di_{sq}}{dt} = -\frac{R_s}{L_s} i_{sq} - n_p \omega_m i_{sd} + \frac{n_p \omega_m}{L_s} \phi_m - \frac{V_s i_{sq}}{L_s \sqrt{{i_{sd}}^2 + {i_{sq}}^2}} \tag{7}$$

$$J \frac{d\omega_m}{dt} = T_w - T_e \tag{8}$$

where $i_{sd}$ and $i_{sq}$ are the stator currents in the $d_q$ frame. $R_s$ is the stator resistance. $L_s$ is the stator inductance. $\omega_m$ represents the mechanical angular speed. $n_p$ is the number of pole pairs of the PMSG. $\phi_m$ designs the permanent magnet flux. $J$ is the total moment of inertia.

The expression of the electromagnetic torque $T_e$ produced by the generator is given by:

$$T_e = \frac{P_{dc}}{\omega_m} = \frac{V_{dc} I_{dc}}{\omega_m} \tag{9}$$

where $P_{dc}$ is the generated electric power; $V_{dc}$ and $I_{dc}$ are the voltage and the current respectively at the output of the three-phase rectifier.

The equation that describes the relationship between the DC voltage $V_{dc}$ and the terminal $V_s$ is as follows:

$$V_{dc} = \frac{3\sqrt{3}}{\pi} V_s \tag{10}$$

In other hand, the DC current $I_{dc}$ can be expressed by the following equation:

$$I_{dc} = \frac{\pi}{2\sqrt{3}} \sqrt{{i_{sd}}^2 + {i_{sq}}^2} \tag{11}$$

## 2.3 Boost converter model

Static converters are essential components of the variable speed wind power conversion system. They allow operation at variable speed and thus extract the maximum of the power produced by the wind turbine. In this work, we consider a boost converter represented by the following differential equations (Dahech et al., 2017).

$$\begin{aligned} \frac{dV_{dc}}{dt} &= \frac{1}{C_1}\left(I_{dc} - I_L\right) \\ \frac{dI_L}{dt} &= f_1(x) + g_1(x)d(t) \\ \frac{dV_{C2}}{dt} &= f_2(x) + g_2(x)d(t) \end{aligned} \tag{12}$$

where

$$f_1(x) = \frac{V_{dc}}{L} - \frac{R_c}{L\left(1 + \frac{R_c}{R_{ch}}\right)} I_L + \frac{1}{L}\left(\frac{R_c}{R_{ch} + R_c} - 1\right) V_{C2} - \frac{V_D}{L} \tag{13}$$

$$g_1(x) = \frac{R_c}{L\left(1 + \frac{R_c}{R_{ch}}\right)} I_L - \frac{1}{L}\left(\frac{R_c}{R_{ch} + R_c} - 1\right) V_{C2} + \frac{V_D}{L} \tag{14}$$

$$f_2(x) = \frac{1}{C_2\left(1+\frac{R_c}{R_{ch}}\right)} I_L + \frac{1}{C_2\left(R_{ch}+R_c\right)} V_{C2} \tag{15}$$

$$g_2(x) = -\frac{1}{C_2\left(1+\frac{R_c}{R_{ch}}\right)} I_L \tag{16}$$

where the three state variables $V_{dc}$, $I_L$ and $V_{C2}$ are respectively the output voltage of the uncontrolled rectifier, the inductor current and the voltage of the capacitor. $V_D$ is the forward voltage of the power diode; $d$ is the duty ratio of the PWM control input signal; $R_{ch}$ is the load resistance.

In the following, an MPPT control approach, based on the sliding mode theory will be presented. The objective is to control the DC voltage $V_{dc}$ in order to extract the maximum power delivered by the wind system.

## 3 Robust MPPT control design

### *3.1 Determination of $V_{dcref}$*

As follows from Figure 3 shown, there exist an unique optimal tip speed ratio $\lambda_{opt}$ for which the aerodynamic power coefficient is maximum $C_{pmax}$. As a result, the mechanical power extracted from the wind is also maximum. Then, the maximum power captured from the wind can be expressed in term of $\lambda_{opt}$ and $C_{pmax}$ by the following equation.

$$P_{\max} = \frac{1}{2}\rho\pi R^2 V_w^3 C_{p\max}\left(\lambda_{opt}\right) \tag{17}$$

Using equation (4), (17) becomes

$$P_{\max} = \frac{\rho\pi R^5 C_{p\max}}{2\lambda_{opt}^3}\omega_m^3 = K_{opt}\omega_m^3 \tag{18}$$

The control aim is to allow the generated electrical power $P_{dc}$ to reach the maximum power Pmax. Given that $P_{dc} = V_{dc}L_{dc}$, the control objective can be accomplished by regulating the DC voltage $V_{dc}$ at a reference value $V_{dcref}$. The reference voltage $V_{dcref}$ is obtained as follows:

$$V_{dcref} = \frac{P_{\max}}{I_{dc}} = \frac{K_{opt}\omega_m}{I_{dc}} \tag{19}$$

In the following, a non-singular fast terminal sliding mode controller is presented for regulating the DC voltage at the output of the uncontrolled rectifier in order to extract the maximum power captured from the wind energy.

### 3.2 Control law design

Consider $e_1$ the error between $V_{dc}$ and $V_{dcref}$:

$$e_1 = V_{dc} - V_{dcref} \tag{20}$$

The derivative of $e_1$ with respect to time is given by:

$$\frac{de_1}{dt} = \frac{dV_{dc}}{dt} - \frac{dV_{dcref}}{dt} = \frac{1}{C_1}\left(-I_L + I_{dc}\right) - \frac{dV_{dcref}}{dt} \tag{21}$$

By introducing the auxiliary error $e_2 = I_L - I_{Lref}$, where $I_{Lref} = I_{dc} - C_1 \frac{dV_{dcref}}{dt}$, equation (21) can be written in another way:

$$\frac{de_1}{dt} = -\frac{e_2}{C_1} \tag{22}$$

Now, by making the changes of variable $z_1 = e_1$ and $z_2 = -\frac{e_2}{C_1}$, we obtain the following second order system:

$$\begin{aligned} \frac{dz_1}{dt} &= z_2 \\ \frac{dz_2}{dt} &= f_3(x) + g_3(x)d(t) \end{aligned} \tag{23}$$

where, $f_3(x) = -\frac{1}{C_1}\left[f_1(x) - \frac{dI_{Lref}}{dt}\right]$ and $g_3(x) = -\frac{g_1(x)}{C_1}$.

Consider the following non-singular fast terminal sliding mode surface $S$:

$$S = z_1 + k_1 z_1^{\gamma} + k_2 z_2^{p/q} \tag{24}$$

where $k_1$ and $k_2$ are two positive constants. $\gamma$, $p$ and $q$ verify $1 < p/q < 2$ and $\gamma > p/q$.

Deriving S with respect to time, we get:

$$\begin{aligned} \frac{dS}{dt} &= \frac{dz_1}{dt} + \gamma k_1 z_1^{\gamma-1}\frac{dz_1}{dt} + k_2 z_2^{p/q-1}\frac{dz_2}{dt} \\ &= z_2 + \gamma k_1 z_1^{\gamma-1} z_2 + k_2\left(p/q\right) z_2^{p/q-1}\left[f_3(x) + g_3(x)d(t)\right] \end{aligned} \tag{25}$$

By setting $\frac{dS}{dt} = 0$, the equivalent control law $d_{eq}(t)$ is deduced as follows:

$$d_{eq}(t) = -\frac{1}{g_3(x)}\left[\frac{1}{k_2}\frac{q}{p} z_2^{2-p/q} + \gamma\frac{k_1}{k_2}\frac{q}{p} z_1^{\gamma-1} z_2^{2-p/q} + f_3(x)\right] \tag{26}$$

The reaching law is selected as:

$$d_{sw}(t) = -\frac{1}{g_3(x)} K sign(S) \tag{27}$$

where $K$ is a positive constant.

Thus, the global control law is designed as:

$$\begin{aligned} d(t) &= d_{eq}(t) + d_{sw}(t) \\ &= -\frac{1}{g_3(x)}\left[\frac{1}{k_2}\frac{q}{p} z_2{}^{2-p/q} + \gamma \frac{k_1}{k_2}\frac{q}{p} z_1{}^{\gamma-1} z_2{}^{2-p/q} + f_3(x) + Ksign(S)\right] \end{aligned} \tag{28}$$

Then, the essential outcome of the NFTSMC is stated by the following theorem 1.

*Theorem 1:* Consider the overall WECS (1–8) and (12). If the sliding surface is chosen as (24) and the NFTSMC is designed as (28), then the DC reference voltage $V_{dcref}$ is tracked in finite time $t_s$.

*Proof:* To study the stability of the proposed MPPT algorithm, we adopt a Lyapunov function candidate as follows:

$$V = \frac{1}{2} S^2 \tag{29}$$

The time derivative of $V$ leads to:

$$\frac{dV}{dt} = S\frac{dS}{dt} = S\left[z_2 + \gamma k_1 z_1{}^{\gamma-1} z_2 + k_2 (p/q) z_2{}^{p/q-1}\left[f_3(x) + g_3(x) d(t)\right]\right] \tag{30}$$

Inserting (28) into (30), we obtain:

$$\frac{dV}{dt} = -S\left[k_2 (p/q) z_2{}^{p/q-1} Ksign(S)\right] \tag{31}$$

since $z_2^{p/q-1}$ for $z_2 \neq 0$, the Lyapunov function assures the following inequality:

$$\dot{V} \leq -k_2 K (p/q) z_2{}^{p/q-1} |S| < -\mu |S| \tag{32}$$

Referring to He et al. (2014) and Xiong et al. (2014), the finite time convergence $t_s$ to the sliding surface (24) can be evaluated as follows:

$$t_s = \int_0^{|z_1(0)|} \frac{(k_2)^{q/p}}{\left(z_1 + k_1 |z_1|^{\gamma}\right)^{q/p}} dz_1 \tag{31}$$

According to Yang and Yang (2011), The finite integration of (31) can be obtained by the gauss hypergeometric function (Abramowitz and Stegun, 1972).

### *3.3 Robustness study*

To evaluate the robustness of the controller in the presence of uncertainties, we consider that the functions $f_3(x)$ and $g_3(x)$ are subject to uncertainties as follows:

$$\begin{aligned} f_3(x) &= \hat{f}_3(x) + \Delta f_3 \\ g_3(x) &= \hat{g}_3(x) + \Delta g_3 \end{aligned} \tag{32}$$

where, $\left(\hat{f}_3;\hat{g}_3\right)$ and ($\Delta f_3$, $\Delta g_3$) are the nominal parts and the uncertain parts of $f_3$ and $g_3$ respectively. We assume that these uncertainties verify the following conditions:

$$\begin{aligned}&\left|\Delta f_3\right| < F_3\\&\sigma^{-1} \le \hat{g}_3/g_3 \le \sigma\end{aligned} \tag{33}$$

Using (32), the time derivative of the sliding surface (24) yields to:

$$\begin{aligned}\frac{dS}{dt} &= \frac{dz_1}{dt} + \gamma k_1 z_1^{\gamma-1}\frac{dz_1}{dt} + k_2 z_2^{p/q-1}\frac{dz_2}{dt}\\&= z_2 + \gamma k_1 z_1^{\gamma-1} z_2 + k_2(p/q) z_2^{p/q-1}\left[\hat{f}_3(x) + \Delta f_3 + \left(\hat{g}_3(x) + \Delta g_3\right) d(t)\right]\end{aligned} \tag{34}$$

Then, the novel NFTSMC in the presence of uncertainties is given by:

$$d(t) = -\frac{1}{\hat{g}_3(x)}\left[\frac{1}{k_2}\frac{q}{p} z_2^{2-p/q} + \gamma\frac{k_1}{k_2}\frac{q}{p} z_1^{\gamma-1} z_2^{2-p/q} + \hat{f}_3(x) + K^* sign(S)\right] \tag{35}$$

Thus, the robustness of the NFTSMC against uncertainties is satisfied via the following theorem 2.

*Theorem 2:* Consider the overall uncertain WECS (1–8) and (12). If the sliding surface is chosen as (24) and the NFTSMC is designed as (35) with a controller gain $K^*$ satisfying the inequality (36), then the DC reference voltage $V_{dcref}$ is tracked in finite time and the maximum power point of the system is achieved.

$$K^* > \frac{|\sigma - 1|\left[\frac{1}{k_2}\frac{q}{p}\left|z_2^{2-p/q}\right| + \gamma\frac{k_1}{k_2}\frac{q}{p}\left|z_1^{\gamma-1}\right|\left|z_2^{2-p/q}\right| + \left|\hat{f}_3\right|\right] + \left|\Delta f_3\right| + \mu}{\frac{p}{q} k_2 \sigma^{-1}} \tag{36}$$

*Proof:* To prove theorem 2, we choose the candidate Lyapunov function $V = \frac{1}{2}S^2$. The derivative of $V$ with respect to time is obtained as:

$$\begin{aligned}\frac{dV}{dt} &= S\frac{dS}{dt}\\&= S\left\{z_2 + \gamma k_1 z_1^{\gamma-1} z_2 + k_2(p/q) z_2^{p/q-1}\left[\hat{f}_3(x) + \Delta f_3 + \left(\hat{g}_3(x) + \Delta g_3\right) d(t)\right]\right\}\end{aligned} \tag{37}$$

Substituting (35) into (37), the above equation can be written as:

$$\begin{aligned}\dot{V} \le\ & -\mu k_2(p/q)|S|\left|z_2^{p/q-1}\right|\\&+ k_2(p/q)|S|\left|z_2^{p/q-1}\right||\sigma - 1|\left(\frac{1}{k_2}\frac{q}{p}\left|z_2^{2-p/q}\right| + \gamma\frac{k_1}{k_2}\frac{q}{p}\left|z_1^{\gamma-1}\right|\left|z_2^{2-p/q}\right| + \left|\hat{f}_3\right|\right)\\&+ k_2(p/q)|S|\left|z_2^{p/q-1}\right|\left(\left|\Delta f_3\right| + \mu\right) - k_2(p/q)K^*\sigma^{-1}|S|\left|z_2^{p/q-1}\right|\end{aligned} \tag{38}$$

Then, the following inequality is derived:

$$\begin{aligned}\dot{V} \le & -\mu k_2(p/q)|S|\left|z_2{}^{p/q-1}\right| \\ & + k_2(p/q)|S|\left|z_2{}^{p/q-1}\right|\left|\sigma - 1\right|\left(\frac{1}{k_2}\frac{q}{p}\left|z_2{}^{2-p/q}\right| + \gamma\frac{k_1}{k_2}\frac{q}{p}\left|z_1{}^{\gamma-1}\right|\left|z_2{}^{2-p/q}\right| + \left|\hat{f}_3\right|\right) \\ & + (p/q)|S|\left|z_2{}^{p/q-1}\right|\left(\left|\Delta f_3\right| + \mu\right) - k_2(p/q)K^*\sigma^{-1}|S|\left|z_2{}^{p/q-1}\right|\end{aligned} \tag{39}$$

Therefore, if the condition (36) is verified, then $\frac{dV}{dt} \le -\mu k_2(p/q)|S|\left|z_2{}^{p/q-1}\right|$. Consequently, $z_1$ and $z_2$ converge to zero in finite time. Thus, $e_1$ and $e_2$ converge also to zero. As a result, the NFTSMC is able to extract maximum power captured from the WECS.

## 4 Simulation results and discussions

In this section, numerical simulations have been performed verifying the effectiveness of the developed MPPT approach. The wind speed is varied to test the operation of the proposed controller under various climatic conditions. The tested system is composed of a wind turbine coupled to a PMSG. A diode bridge is used for rectifying the output voltage of the PMSG. A boost converter is used to track the MPP of the wind turbine by adjusting the DC voltage at the output of the rectifier. The simulation parameters of the wind system and the control law are summarised in Table 1.

**Table 1** Simulation parameters

| *Wind turbine* | *PMSG* | *Boost converter* | *Control law* |
|---|---|---|---|
| $\rho = 1.205\,Kg/m^3$ | $R_s = 0.57\Omega$ | $C_1 = 1mF; C_2 = 1mF$ | $k_1 = 5; k_2 = 7; K = 10$ |
| $R = 1.74\,m$ | $L_s = 0.55mH$ | $L = 1.2mH; R_c = 2\Omega$ | $p = 9; q = 5; \gamma = 3$ |
| $\lambda_{opt} = 6.9$ | $\phi_m = 0.196Wb$ | $V_D = 0.7V; R_{ch} = 25\Omega$ | |
| $C_{p\max} = 0.47$ | $n_p = 4$ | | |
| | $J = 0.0164Kg.m^2$ | | |
| | Rated power: $6.4kW$ | | |

We first adopt a variable wind profile over three stages. Indeed, a step of wind speed (increase from 6 *m/s* to 10 *m/s* then a decrease to 7 *m/s*) is applied to the wind turbine, Figure 4. The simulation results relating to this first test are illustrated in Figures 5 to 10. By examining Figure 5, we note that the DC voltage $V_{dc}$ follows its reference value $V_{dcref}$ corresponding to each step of the wind speed. The evolution of $V_{dc}$ is characterised by a transient without overshooting and oscillation. In addition, it can be seen from Figures 6 and 7 that the convergence of the voltage $V_{dc}$ causes an immediate convergence of the rotational speed $\omega_m$ and the power $P_{dc}$ to their optimal values. Moreover, the aerodynamic power coefficient is maintained at its maximum value $C_{pmax}$, Figure 8. As can be seen from Figures 9 and 10, the nonsingular fast terminal sliding mode controller shows improved reliability and remarkable chattering reduction. It can be conclude that the turbine mechanical power follow the optimum power curve quite well and the generator can extract maximum power under variable wind speeds.

**Figure 4** Step change of wind speed (see online version for colours)

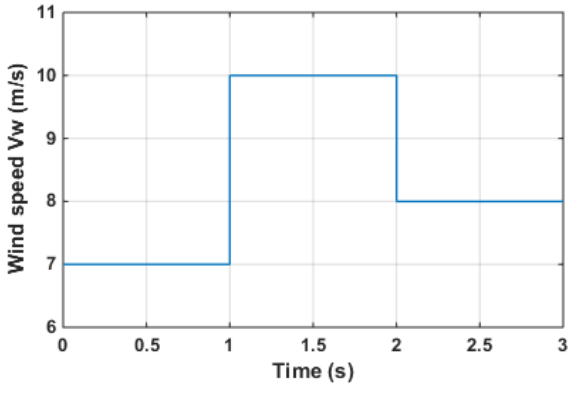


**Figure 5** Evolution of $V_{dc}$ and $V_{dcref}$ (see online version for colours)

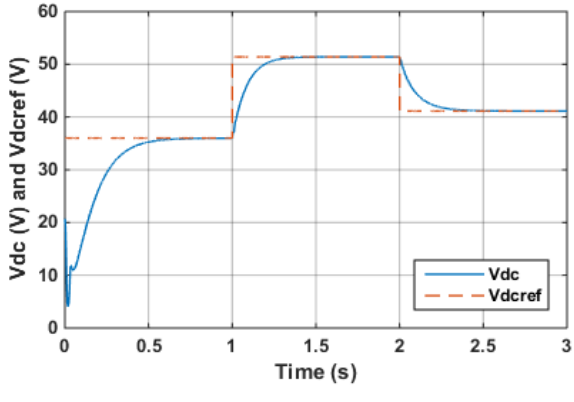


**Figure 6** Evolution of $\omega_m$ (see online version for colours)

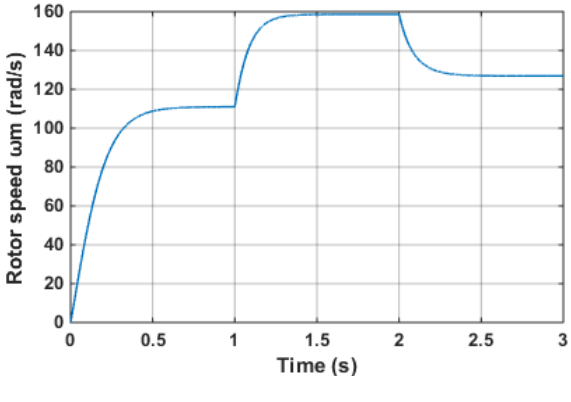

**Figure 7** Evolution of $P_{dc}$ and $P_w$ (see online version for colours)

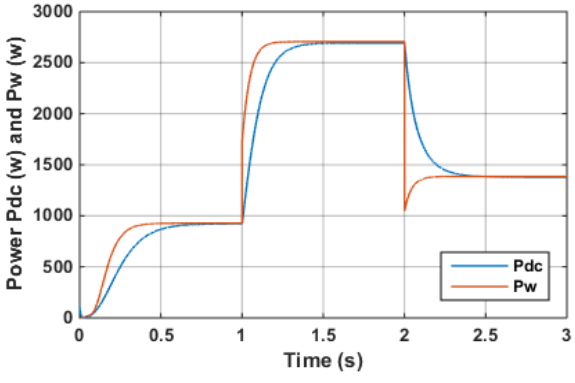


**Figure 8** Evolution of $C_p(\lambda)$ (see online version for colours)

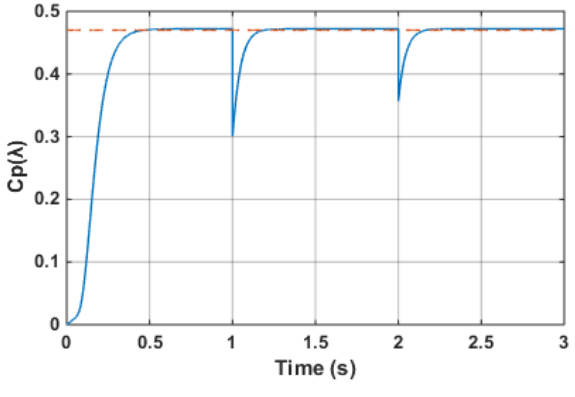


**Figure 9** Control law $d(t)$ (see online version for colours)

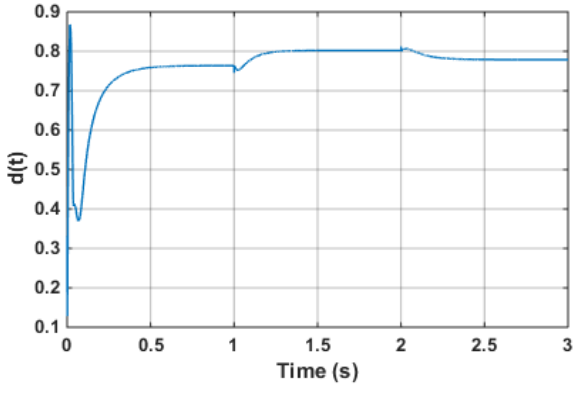

**Figure 10** Sliding surface $S$ (see online version for colours)

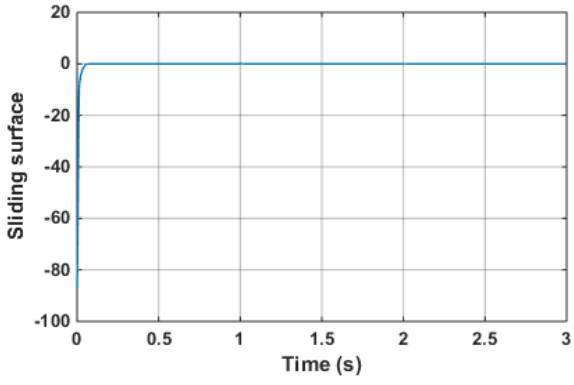


As a second scenario, we choose a wind profile that varies between 4 *m/s* and 8.5 *m/s* presented in Figure 11. It can be seen from Figures 12 to 17 that the developed control law has good performance in terms of tracking the different trajectories regardless the fluctuating nature of the wind speed. Besides, it is obvious to note that the aerodynamic power coefficient $C_p$ presents small fluctuations in the vicinity of its maximum value $C_{pmax}$. This shows that the power extracted is optimised.

**Figure 11** Wind speed profile (see online version for colours)

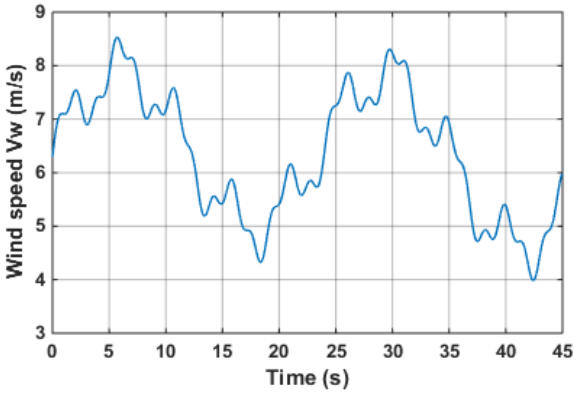


A comparative study is performed between the proposed NFTSMC and the classical sliding mode controller (SMC) in term of power error tracking ($P_{max}$–$P_{dc}$). For simulation, the traditional sliding mode controller is obtained by setting ($\gamma = 1$; $p = q$) in the sliding function (24). Simulation results are shown in Figure 18. the application of the classical sliding mode controller generates a higher error rate of tracking than the NFTSMC.

**Figure 12** Evolution of $V_{dc}$ and $V_{dcref}$ for variable wind speed (see online version for colours)

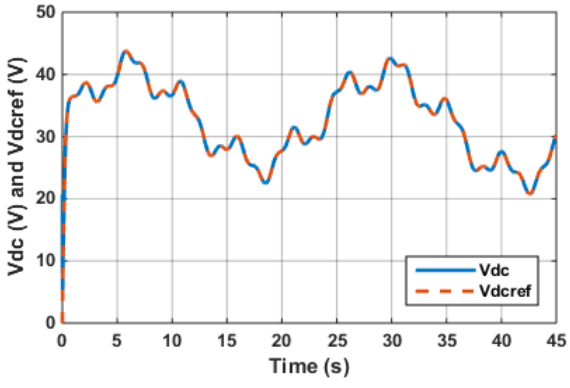


**Figure 13** Evolution of $\omega_m$ for variable wind speed (see online version for colours)

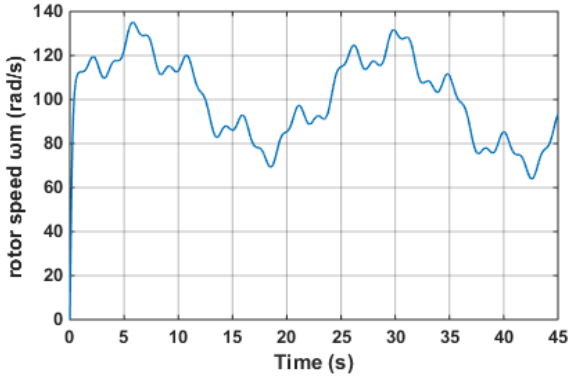


**Figure 14** Evolution of $P_{dc}$ and $P_w$ for variable wind speed (see online version for colours)

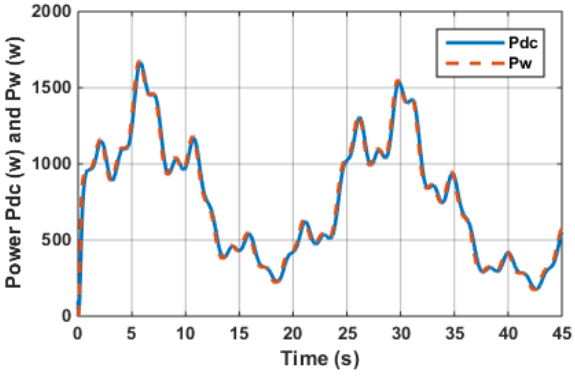

**Figure 15** Evolution of $C_p(\lambda)$ for variable wind speed (see online version for colours)

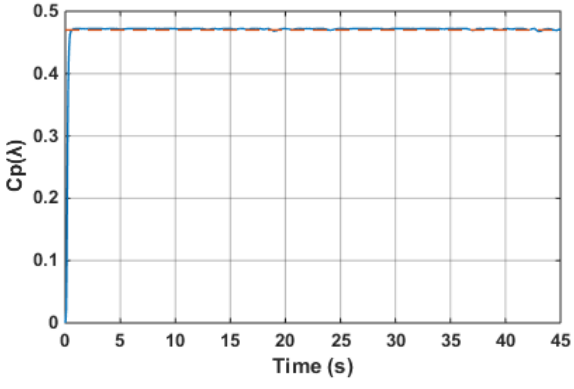


**Figure 16** Evolution of $d(t)$ for variable wind speed (see online version for colours)

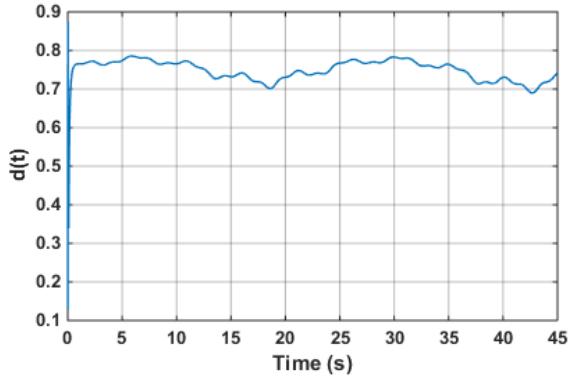


**Figure 17** Evolution of the sliding surface $S$ (see online version for colours)

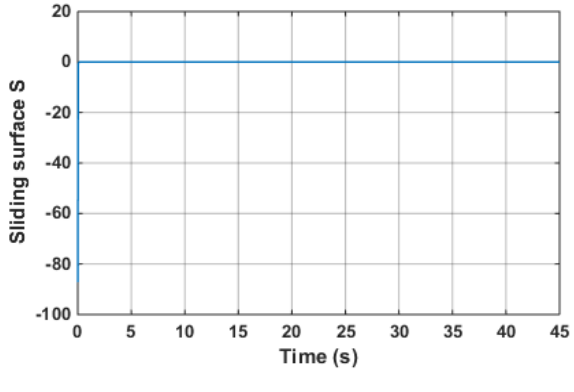

**Figure 18** Power error tracking ($P_{max}$–$P_{dc}$) (see online version for colours)

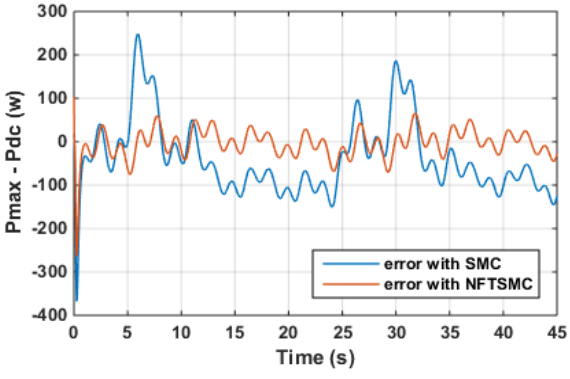


These simulation results show that the non-singular fast terminal sliding mode controller works very well. He ensured the tracking of the MPP under all variations in climatic conditions with precision and speed.

## 5 Conclusions

A non-singular fast terminal sliding mode control approach for maximum power point tracking of a wind energy conversion system is presented. The controlled system used in this work consists of a permanent magnet synchronous generator connected to a three-phase diode rectifier with a DC-DC boost converter and a resistive load. Thanks to this architecture, the MPPT control algorithm studied has been implemented using only the DC voltage and the DC current measurements at the output of the rectifier, thus avoiding the presence of mechanical measurement devices. The efficiency of the proposed MPPT technique has been proved by simulation studies under two wind profiles. All the collected results are very convincing and attest that the behaviour of the system with this algorithm is significantly improved. Indeed, the proposed approach presents a good transition response without overshoot, a low tracking error and a fast system reaction against wind speed change. The benefit of the proposed NFTSMC, compared to the classical SMC, is the good power error tracking, the chattering reduction and the finite time convergence. Consequently, the approach ensured a good tracking of MPP, despite variations in climatic conditions.

## References

Abderrahim, S., Allouche, M. and Chaabane, M. (2020) 'A New Robust Control Strategy for a Wind Energy Conversion System Based on a TS Fuzzy Model', *International Journal of Smart Grid*, Vol. 4, No. 2, pp.88–99.

Abderrahim, S., Allouche, M. and Chaabane, M. (2021) 'Power optimisation of wind energy conversion system using T-S fuzzy approach', *International Journal of Industrial and Systems Engineering*, Vol. 38, No. 1, pp.35–58.

Abdullah, M.A., Yatim, A.H.M., Tan, C.W. et al. (2012) 'Review of maximum power point tracking algorithms for wind energy systems', *Renewable and Sustainable Energy Reviews*, Vol. 16, No. 5, pp.3220–3227.

Abolvafaei, M. and Ganjefar, S. (2019) 'Maximum power extraction from a wind turbine using second-order fast terminal sliding mode control', *Renewable Energy*, Vol. 139, No. 1, pp.1437–1446.

Abolvafaei, M. and Ganjefar, S. (2021) 'Two novel approaches to capture the maximum power from variable speed wind turbines using optimal fractional high-order fast terminal sliding mode control', *European Journal of Control*, Vol. 60, No. 1, pp.78–94.

Abramowitz, M. and Stegun, I.A. (1972) *Handbook of Mathematical Functions: with Formulas, Graphs, and Mathematical Tables*, Dover: New York, USA.

Allouche, M., Abderrahim, S., Ben Zina, H. et al. (2019) 'A novel fuzzy control strategy for maximum power point tracking of wind energy conversion system', *International Journal of Smart Grid*, Vol. 3, No. 3, pp.120–127.

Ardjal, A., Mansouri, R. and Bettayeb, M. (2018) 'Fractional sliding mode control of wind turbine for maximum power point tracking', *Transactions of the Institute of Measurement and Control*, Vol. 41, No. 2, pp.447–457.

Chiu, C.S., Chiang, T.S., Chou, M.L. et al. (2014) 'Maximum power point tracking of wind power systems via fast terminal sliding mode control', In *11th IEEE International Conference on Control and Automation* (ICCA), Taichung, Taiwan, June 18–20.

Chiu, C.S., Li, Z.H. and Chen, Y.H. (2013) 'T-S fuzzy direct maximum power point tracking of wind energy conversion systems', *International Journal of Fuzzy Systems*, Vol. 15, No. 2, pp.192–202.

Dahech, K., Allouche, M., Damak, T. et al. (2017) 'Backstepping sliding mode control for maximum power point tracking of a photovoltaic system', *Electric Power Systems Research*, Vol. 143, No. 1, pp.182–188.

Daili, Y., Gaubert, J.P. and Rahmani, L. (2015) 'Implementation of a new maximum power point tracking control strategy for small wind energy conversion systems without mechanical sensors', *Energy Conversion and Management*, Vol. 97, No. 1, pp.298–306.

Evangelista, C.A., Pisano, A., Puleston, P. et al. (2017) 'Receding horizon adaptive second-order sliding mode control for doubly-fed induction generator based wind turbine', *IEEE Transactions on Control Systems Technology*, Vol. 25, No. 1, pp.73–84.

Gam, O., Abdelati, R., Tankari, M.A. et al (2019) 'An improved energy management and control strategy for wind water pumping system', *Transactions of the Institute of Measurement and Control*, Vol. 41, No. 14, pp.3921–3935.

Hau, E. (2013) *Wind Turbines Fundamentals, Technologies, Application, Economics*, Third, translated edition, Springer-Verlag Berlin Heidelberg.

He, Z., Liu, C., Zhan, Y., Li, H. et al. (2014) 'Nonsingular fast terminal sliding mode control with extended state observer and tracking differentiator for uncertain nonlinear systems', *Hindawi Publishing Corporation Mathematical Problems in Engineering 2014*.

Hostettler, J. and Wang, X. (2015) 'Sliding mode control of a permanent magnet synchronous generator for variable speed wind energy conversion systems', *Systems Science and Control Engineering*, Vol. 3, No. 1, pp.453–459.

Jayshree, P., Paresh, N., Ketan, K. and Vijayakumar, V. (2021) 'A review of maximum power point tracking algorithms for wind energy conversion systems', *Journal of Marine Science and Engineering*, Vol. 9, No. 11, pp.158–188.

Kesraoui, M., Korichi, N. and Belkadi, A. (2011) 'Maximum power point tracker of wind energy conversion system', *Renewable Energy*, Vol. 36, No. 10, pp.2655–2662.

Kumar, D. and Chatterjee, K. (2016) 'A review of conventional and advanced MPPT algorithms for wind energy systems', *Renewable and Sustainable Energy Reviews*, Vol. 55, No. 1, pp.957–970.

Kumar, S.S. and Selvakumar, A.I. (2020) 'Maximum power point tracking and power flow management of hybrid renewable energy system with partial shading capability: a hybrid technique', *Transactions of the Institute of Measurement and Control*, Vol. 42, No. 12, pp.2276–2296.

Mousa, H., Youssef, A.R. and Mohamed, E.E.M. (2020) 'Hybrid and adaptive sectors P&O MPPT algorithm based wind generation system', *Renewable Energy*, Vol. 145, No. 1, pp.1412–1429.

Nasiri, M., Milimonfared, J. and Fathi, S.H. (2014) 'Modeling, analysis and comparison of TSR and OTC methods for MPPT and power smoothing in permanent magnet synchronous generator-based wind turbines', *Energy Conversion and Management*, Vol. 86, No. 1, pp.892–900.

Ruban periyanayagam, A. and Joo, Y.H. (2022) 'Integral sliding mode control for increasing maximum power extraction efficiency of variable-speed wind energy system', *International Journal of Electrical Power and Energy Systems*, Vol. 139, No. 1, pp.588–600.

Xiong, L., Li, P. and Wang, J. (2020) 'High-order sliding mode control of DFIG under unbalanced grid voltage conditions', *Electrical Power and Energy Systems*, Vol. 117, No. 1, pp.436–448.

Xiong, S.F., Wang, W.H. and Wang, S. (2014) 'Nonsingular fast terminal sliding-mode guidance with intercept angle constraint', *Control Theory and Applications*, Vol. 31, No. 3, pp.269–278.

Yang, L. and Yang, J. (2011) 'Nonsingular fast terminal sliding-mode control for nonlinear dynamical systems', *International Journal of Robust and Nonlinear Control*, Vol. 21, No. 16, pp.1865–1879.

Yazici, İ. and Yaylaci, E.K. (2019) 'Discrete-time integral terminal sliding mode based maximum power point controller for the PMSG-based wind energy system', *IET Power Electron*, Vol. 12, No. 14, pp. 3688–3696.

Yin, X., Jiang, Z. and Pan, L. (2020) 'Recurrent neural network based adaptive integral sliding mode power maximization control for wind power systems', *Renewable Energy*, Vol. 145, No. 1, pp.1149–1157.

Yin, X., Lin, Y., Li, W. et al. (2015) 'Sliding mode voltage control strategy for capturing maximum wind energy based on fuzzy logic control', *Electrical Power and Energy Systems*, Vol. 70, No. 1, pp.45–51.

Zhuo, G., Hostettler, J.D., Gu, P. et al. (2016) 'Robust sliding mode control of permanent magnet synchronous generator-based wind energy conversion systems', *Sustainability*, Vol. 8, No. 12, pp.163–178.